THE USE OF 1H NMR: A NEW METHOD TO ADDRESS THE PROPERTIES OF CONCRETES

A.C.A. Muller[1], K.L. Scrivener[1], P.J. McDonald[2]

[1] *Laboratory of Construction Materials, EPFL, Lausanne, Switzerland*
[2] *Department of Physics, University of Surrey, Guildford, Surrey, U.K*

ABSTRACT

Supplementary cementitious materials (SCMs) are more and more used in the field for their cheap price and sometimes their good contributions to the durability of concretes. However, it is difficult to link these properties to fundamental hydrations processes and nano-porosity of the C-S-H. ^{1}H nuclear magnetic resonance (NMR) has been used to fully characterise the water in and the composition of cement paste. Our methodology is quantitative, non invasive and allows C-S-H density and chemical composition to be found with and without the use of SCMs. The resultant ''solid'' C-S-H density and composition are $\rho = 2.7$ g/cm$^{3;}$ $Ca_{1.7}(Si_{0.95},Al_{0.05})O_{3.7}(H_2O)_{1.8}$ for sealed cured white cement paste mixed at *w/c* = 0.4 after 28 days of hydration. The use of silica fume does not change densities of C-S-H but highly impacts water content and Ca/(Si+Al) ratio. Ca/(Si+Al) = 1.25 at 28 days when 10% of silica fume is used. The addition of slag has a strong impact on the gel water and the way hydration products fill space.

INTRODUCTION

Cement production exceeds 3 billion tonnes per annum and globally infrastructure relies massively on concrete. Cement contributes 5-8% of global CO_2 emissions [1] and there is clearly a need to reduce it. A way forward is to incorporate more environmentally favourable supplementary cementitious materials (SCMs). However, these new materials can considerably change the hydration processes and impact the microstructure of cement pastes.

Basic cement hydration involves the dissolution of C_3S and C_2S in water and the formation, by precipitation, of mainly calcium silicate hydrate (C-S-H) and calcium hydroxide (CH in cement notation, also called Portlandite). While calcium hydroxide is a very well known crystalline phase, the structure of C-S-H remains uncertain. The primary reasons are twofold: firstly, C-S-H is a highly disordered nanoscale material incorporating a significant amount of water and hence, difficult to probe experimentally. Only a few techniques are able to adequately characterise as-prepared C-S-H without removing the water: a procedure that damages the nanoscale structures that are of interest. Secondly, the way C-S-H precipitate is highly dependent on the chemical and physical conditions in which the hydration takes place. C-S-H can be highly impacted by the use of SCMs and the different phenomena leading to C-S-H precipitation then become complex. The first requirement for the use of SCMs as a replacement of cement is to maintain concrete properties. Hence, C-S-H chemical composition, density and morphology are of great importance regarding the durability of new cement-based materials.

Since water underpins performance and is central to all concrete degradation mechanisms, progress requires thorough understanding of C-S-H nanostructure and the role of water within it. Nuclear Magnetic Resonance relaxation time analysis is an established technique for non-invasive and non-destructive characterization of pore size distributions and pore-water interaction in porous media such as cement and concrete [2,3]. The objective of this study is to show that the NMR experiment is quantitative, simply to carry out and provide a greater level of detail concerning microstructure than other techniques. We present how quantitative NMR data can lead to the full description of cement paste, C-S-H density and chemical composition. ^{1}H NMR is used to determine the evolution of nanoscale porosity of pure white cement pastes, and in parallel including addition of silica fume and slag. The impact of these SCMs on characteristics of C-S-H is investigated.

METHODS

^{1}H NMR relaxometry

^{1}H NMR probes the water, or more precisely the hydrogen protons, within filled pores. The NMR signal amplitude is proportional to the mass of water and the signal lifetime, known as the spin-spin relaxation time T_2, is proportional to pore size [4]. By applying combined Carr-Purcell-Meiboom-Gill (CPMG) [5] and quadrature solid echo (Quad-Echo) [6] pulse sequences, all hydrogen protons in the cement paste can be measured and quantified in their different environments.

^{1}H NMR measurements were made on a Bruker Minispec NMR spectrometer operating at 7.5 MHz. Both Quad-Echo and CPMG measurements were carried out separately. The quadrature echo signals were deconvoluted into a Gaussian and an exponential decay part. The exponential fraction arises from the mobile water within the sample and is not pulse gap dependent. The Gaussian has a very short time constant, of the order of 10 μs, and is assigned to water in crystalline solid phases Portlandite and Ettringite. Its amplitude was back extrapolated to zero pulse gap free from relaxation phenomena using Gaussian fitting. The mobile part of the signal was separately resolved into different T_2 components using the CPMG intensity decay. For this, the Inverse Laplace Transform (ILT) algorithm developed by Venkataramanan [7] was used. C-S-H interlayer water, C-S-H gel pore water and capillary pore water can be distinguished. More details about the analysis of our ^{1}H NMR relaxation characteristics are given in [8]. For the so-called fast diffusion limit [4] for pores filled with water, the characteristic T_2 of each liquid water component can be interpreted to pore size. T_2 of water in pores of cement paste usually varies from 100μs to 100 ms.

Mixes studied

The primary binder of this study is a white cement provided by Aalborg. It is mainly composed of C_3S (67%) and C_2S (20%), C_3A (3.6%) and 4.7% of sulphate phases with other elements representing less than 1% of the mass. The cement has a density of 3.15 g/cm^3. 80 g of white cement was mixed for 2 minutes at 1600 rpm at w/c = 0.40 in a paste mixer LABORTECHNIK RW 20.n. Small amounts of paste (0.35 cm^3) were deposited at the bottom of NMR glass tubes and sealed with parafilm. Multiple samples cast at different times were intermittently measured in a temperature-controlled ^{1}H NMR probe according to the aforementioned procedure. This plain white cement paste acts as the reference mix.

The second paste studied was white cement paste with incorporation of 10% of silica fume as a mass replacement of cement. The mix was made according to the following procedure: the silica fume was first pre-dispersed in distilled water for 8 minutes at 15 000 rpm in an ultrasonic bath. No superplasticizer was used for rheological or dispersive purposes in order not to introduce more hydrogen signal into the system. Then, the water and suspended silica fume was added to the cement to achieve a water-to-binder ratio of w/b = 0.4 by weight. All components were then mixed together for 5 minutes at 1600 rpm. Condensed silica fume made of 98.6% of amorphous silica was used. It is provided by Elkem under the name “Microsilica 983 U” and has an absolute density of 2.27 g/cm^3.

The last part of this study focuses on the influence of slag. We studied the presence of 10%, 20%, 30%, and 40% of slag by weight. In these 4 cases, the white cement content was kept at 60% with complement of quartz. This was done to keep the same amount of cement and vary the amount of slag at a constant water-to-solid ratio. A mix with 60% of white cement and 40% of quartz was also cast as a reference paste. The slag is made of 41% of CaO, 36% of SiO_2, 12% of Al_2O_3 and 8% of MgO with other minor phases. The quartz is supposed to be inert and has a similar particle size distribution as the slag. The mixing procedure was the same as for plain white cement with 2 minutes at 1600 rpm.

Other samples were independently cast in bigger containers for X-Ray diffraction (XRD). XRD measurements were first done on slices right after cutting while other samples were stopped by immersion in isopropanol for 7 days, vacuum dried, crushed and then measure as a powder. A Panalatical X’Pert Pro MPD diffractometer in a θ-θ configuration was used with a CuKα source (wavelength 1.54 Å) and a fixed divergence slit of 0.5°. Samples were scanned on a rotating stage between 7 and 70° (2θ) using a X’Celerator detector with a step size of 0.0167° (2θ) and a time step of 77.5 s.

All specimens in this study were kept at 20°C throughout the hydration. Pastes are sealed so voids and large pores are present but not filled with water. In order to complete the analysis, the chemical shrinkage volume, not seen by ^{1}H NMR, is required. A conventional technique of measuring chemical shrinkage is used.

Additionally, the degree of reaction of silica fume was measured by ^{29}Si MAS NMR. The solid-state ^{29}Si MAS NMR spectra were recorded at two different magnetic field strengths (7.1 T and 9.4 T) on Varian Unity INOVA-300 and -400 spectrometers, using home-built CP/MAS probes designed for 7, 5, or 4 mm o.d. rotors with sample volumes of 220, 110, and 80 µL, respectively.

STUDY OF PLAIN WHITE CEMENT

Based on the different NMR signals, the mass of water in the different environments of cement paste can be quantified at any measurement time. We distinguish: water in the crystalline phases Portlandite and Ettringite (with NMR signal fraction I_{solid}); water in C-S-H interlayer (I_{CSH}); water in CSH gel (I_{gel}) and water in capillary pores (I_{cap}). All signal fractions add up to unity as $I_{solid} + I_{CSH} + I_{gel} + I_{cap} = 1$. Measurements were done from mixing up to 300 days of hydration. Throughout mass balance and oxides conservation equations C-S-H chemical composition can be found; volume balance gives C-S-H density [8]. Assembling the data, mass and volume composition of the paste can be drawn against, for instance, degree of hydration, updating Powers and Brownyard's well-known model from 1948 [9]. The calculated volumes are presented in figure 1a. The data points appear in black on the diagram.

The way NMR sees separately C-S-H interlayer water and C-S-H gel water allow us to considered separately what we call "solid" and "bulk" C-S-H [8]. The "solid" C-S-H includes the Ca−O backbone layers with SiO_2 tetrahedra plus the interlayer water in between. The red rectangle on the figure illustrates schematically the area defining "solid" C-S-H. The "bulk" C-S-H stands for the overall C-S-H phase inclusive of the gel water (green rectangle on the figure). The evolution of the calculated C-S-H density, inclusive and exclusive of gel water is presented in the Figure 1b.

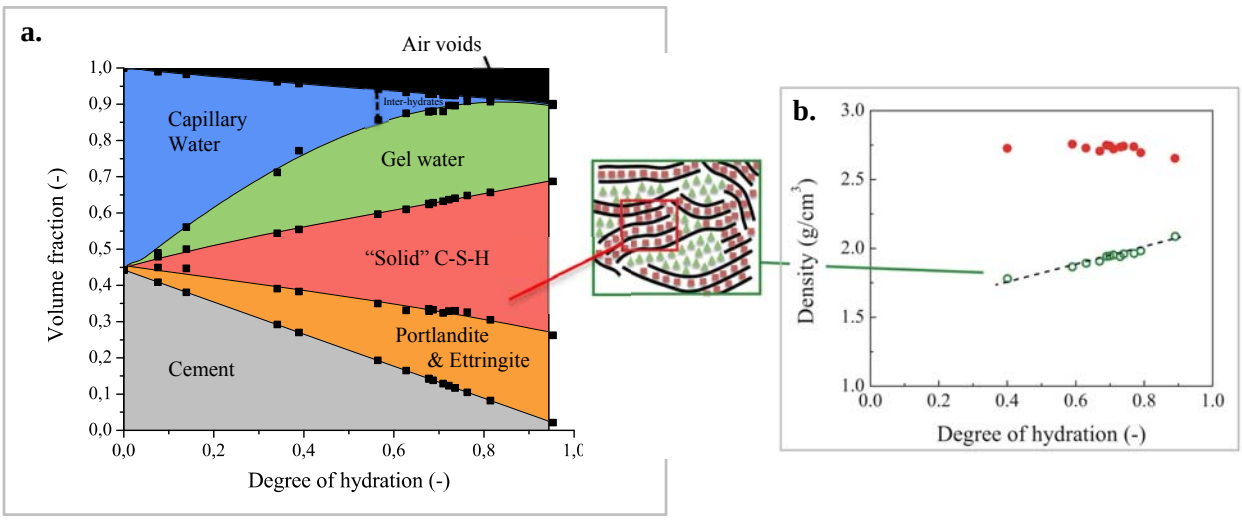

Figure 1 – (a) Volume composition of white cement paste at w/c = 0.4 as a function of degree of hydration of cement. (b) Associated C-S-H densities exclusive of the gel water (red dots) and for the "bulk" C-S-H (green empty dots). There is a schematic representation of the C-S-H water as seeing by NMR. Small red squares are interlayer water and green triangles are gel water, all within C-S-H hydrates.

The diagram shows the continuous consumption of cement and capillary water leading to the formation of hydration products. Portlandite, Ettringite and C-S-H amounts increase with time. The capillary water rapidly goes down with degree of hydration. At 2.2 day of hydration ($\alpha_c = 0.6$), the T_2 of these capillary reservoirs becomes stable at 1 ms [8]. This relaxation time corresponds to a pore diameter of circa 8 nm. After 2.2 days, the capillary water continues to be consumed to form more hydration products but no further decrease in size

is observed. Based on this fact, beyond 2.2 days of hydration, we rename the capillary spaces "interhydrate" spaces as we believe that 8 nm is the distance between the growing C-S-H needles. In parallel, calculations give 0.85 nm for the C-S-H interlayer spacing and 2.5 nm for the C-S-H gel reservoirs. More discussion can be found in reference [8].

The main difference between our diagram based on NMR signals and Powers' model is the non-linear behaviour of the gel water with degree of hydration. The C-S-H gels are formed mainly during the first 2 days of hydration and then plateaus. This highlights a densification of the "bulk" C-S-H (inclusive of the gel water) with time. Figure 1b displays the rate of this densification, with density increasing from 1.7 g/cm^3 at 1 day up to 2.1 g/cm^3 at 300 days. On another hand, the "solid" density of C-S-H layers (exclusive of the gel water) is constant with time at around ρ_{solid} = 2.7 g/cm^3. This value is close to already reported data [10]. The average "solid" C-S-H chemical composition is found to be $Ca_{1.7}(Si_{0.95},Al_{0.05})O_{3.7}(H_2O)_{1.8}$ for high degree of hydration. This is equally in agreement with previously reported data in the literature [11,12].

INFLUENCE OF SILICA FUME

The addition of 10% of silica fume is known to change the microstructure of concretes. There are several reasons: chemical effect of silica fume on the pore solution, filler effects due to its very small size or change in the morphology when C-S-H precipitates from the pozzolanic reaction. Many studies focus on the changes due to addition of silica fume. Some authors have tried to quantify C-S-H composition in the presence of silica fume based on non-evaporable water measured by TGA using chemical equilibrium [13,14]. The C/S ratio is know to decrease with addition of silica fume leading to a decrease in C-S-H water content within the interlayer space [15]. However, there is no clear/full description on the changes happening to the nanostructure of C-S-H in never dried systems as the hydration proceeds.

Following the same procedure as for the plain white cement, we have used ^{1}H NMR to characterise the evolution of white cement paste incorporating 10% of silica fume. The evolution of the signal fractions of the different populations of mobile water is presented in Figure 3a. Interlayer water signals are red squares (I_{CSH}), gel signal fractions are green triangles (I_{gel}) and capillary water blue circles (I_{cap}). For clarity of the graph, the solid signal I_{solid} accounting for crystalline phases is not shown in this figure. Coloured symbols are for white cement + 10% of silica fume, which is compared to plain white cement (grey symbols). The associated T_2 relaxation times are shown in figure 3b; symbols are the same as in Figure 3 (a).

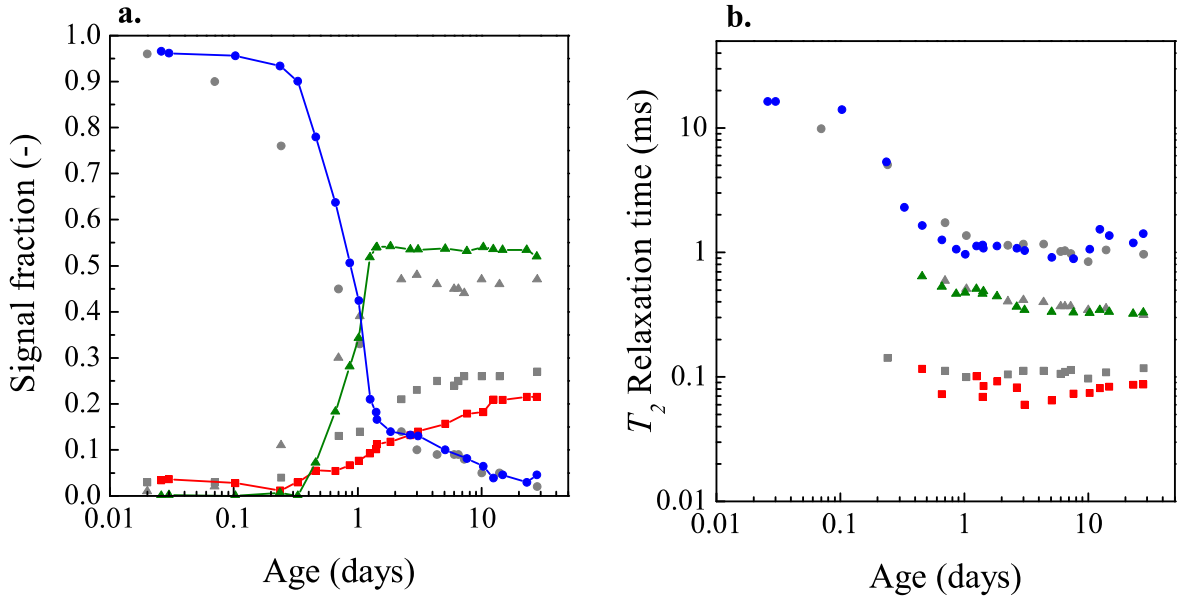

Figure 3 – (a) Evolution of the different mobile water populations against time for white cement + 10% silica fume (colours) and for the reference plain white cement (black), all at w/b = 0.4. Rounds are capillary water signals, squares C-S-H interlayer water signals and triangles are C-S-H gel water signals. The NMR solid

signal is not shown on this graph. (b) Evolution of the associated T_2 relaxation times for the different water populations. Symbols are in accordance with signal amplitudes.

The cement with silica fume behaves very similarly to plain white cement. However, there are important differences.

The first difference is that the end of gel pores formation happens earlier, at about 1 day for the silica fume mix compared to 2.2 days observed for plain white cement paste. This time coincides with the moment when of the capillary spaces reaches 8 nm, the interhydrate specific size. This is compatible with the acceleration of the hydration of the clinker phases by silica fume as widely reported by others and seen in our calorimetry studies. The rate of reaction and nature of C-S-H precipitation seems to be controlled by space filling, as already proposed by Bishnoi et al. [16]. The results of XRD measurements and Rietveld quantification give $\alpha_c = 0.52$ at 1 day of hydration compared to $\alpha_c = 0.40$ observed for plain white cement at the same age. This increased hydration is explained by the extra surface provided by the silica fume, acting as nucleation sites for C-S-H to form [17].

The second difference is that the fraction of C-S-H interlayer water is 30% lower in the presence of silica fume. In parallel, the gel water fraction increases and quickly represents more half of all the water in the paste. The silica fume favours the formation of gel pores. Despite this change in amount, the gel pore size is identical to in the plain white cement paste as shown by the same T_2 relaxation times seeing in figure 3b. We note that the capillary/interhydrate population is of similar amount and size for both mixes.

The shortest T_2 relaxation times observed for the interlayer spacing suggests a smaller interlayer space for the silica fume mix. However, the interpretation from T_2 to pore size for the C-S-H interlayer is difficult to substantiate. The pore size interpretation is based upon the fast diffusion model of relaxation which pre-supposes the existence of a surface layer water and bulk pore water. In such a small place, this model is of limited application.

The degree of hydration of silica fume was measured by ^{29}Si NMR. The results shows $\alpha_{sf} = 34\%$ at 3 days, $\alpha_{sf} = 62\%$ at 14 days $\alpha_{sf} = 67\%$ at 28 days of hydration. Combined with XRD results, it allows C-S-H density and chemical composition to be calculated. The C-S-H "bulk" density for the silica fume mix at 28 days, $\rho_{x'} = 1.94$ g/cm^3 is similar to the one calculated for plain white cement at the same hydration age: $\rho_{x'} = 1.96$ g/cm^3. In the same way, the "solid" C-S-H density at 28 days, $\rho_x = 2.75$ g/cm^3, is identical to the one reported for plain white cement [8]. At 28 days, no major change concerning C-S-H density is occurring by the addition of 10% of silica fume. However, chemical composition of the C-S-H is highly impacted. Ca/(Si+Al) ratio and the associated water content are presented in figure 4. The results are presented as a function of time and compared to plain white cement (grey lines).

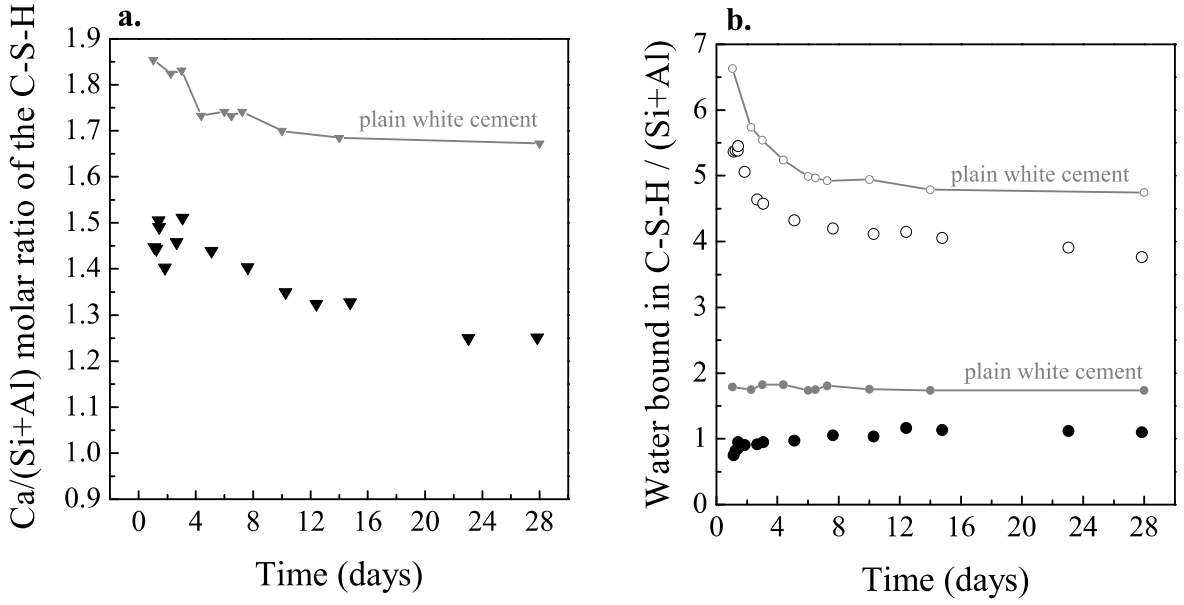

Figure 4 – White cement with 10% silica fume at *w/b* = 0.4 as a function of hydration time. The grey lines in all figures track the behaviour of plain white cement taken from [8] *(a)* Ca/(Si+Al) ratio of the C-S-H calculated from ^{1}H NMR (black inverted triangles). (b) Water content for the "solid" (black circles) and "bulk" (open circles) C-S-H expressed as H_2O/(Si+Al).

For the C-S-H water contents, the main differences here compared to plain white cement are the absolute water contents. The values calculated for 10% of silica fume are significantly lower than without. We report an average "solid" C-S-H water content of x = 1.1 H_2O/(Si+Al) beyond 20 days of hydration. This is a decrease of 39% compare to x = 1.8 for plain white cement. The decrease in H_2O/(Si+Al) ratio is also observed in the case of "bulk" C-S-H. The total water content of C-S-H goes down from x'=5.5 at 1 day of hydration to x'=3.8 at 28 days. We note that the decrease of "bulk" water content with time is a resultant of densification.

We calculate a Ca/(Si+Al) ratio of 1.5 for the first days of hydration which is significantly smaller than for plain white cement with Ca/(Si+Al) = 1.8 at early age (grey line in figure 4a). This substantial decrease seems to occur early in the hydration process due to the presence of silica fume. As the hydration proceeds, this ratio goes progressively down to 1.34 at 28 days. These results are of great importance regarding C-S-H formation as we show that the incorporation of only 10% of silica fume has a strong impact on the chemical composition of C-S-H.

INFLUENCE OF SLAG

The different water populations described in the previous sections were studied with incorporation of 10%, 20%, 30% and 40% of slag by mass over the total solid content. The different pastes were measured at 28 days of hydration. The results are presented in figure 5a as a function of slag content. As a reminder, the solid mass was completed by quartz when the slag content was decreased, keeping the white cement content at 60%. This allows to keep a water-to-solid ratio constant at *w/s* = 0.40 so the same amount of water was probed by ^{1}H NMR.

In order to ascertain the NMR solid signal I_{solid} previously attributed to solely crystalline phases, parallel XRD measurements were done. The crystalline phases Portlandite and Ettringite as measured by diffraction are presented in figure 5b; Hydrotalcite is seen when slag is used.

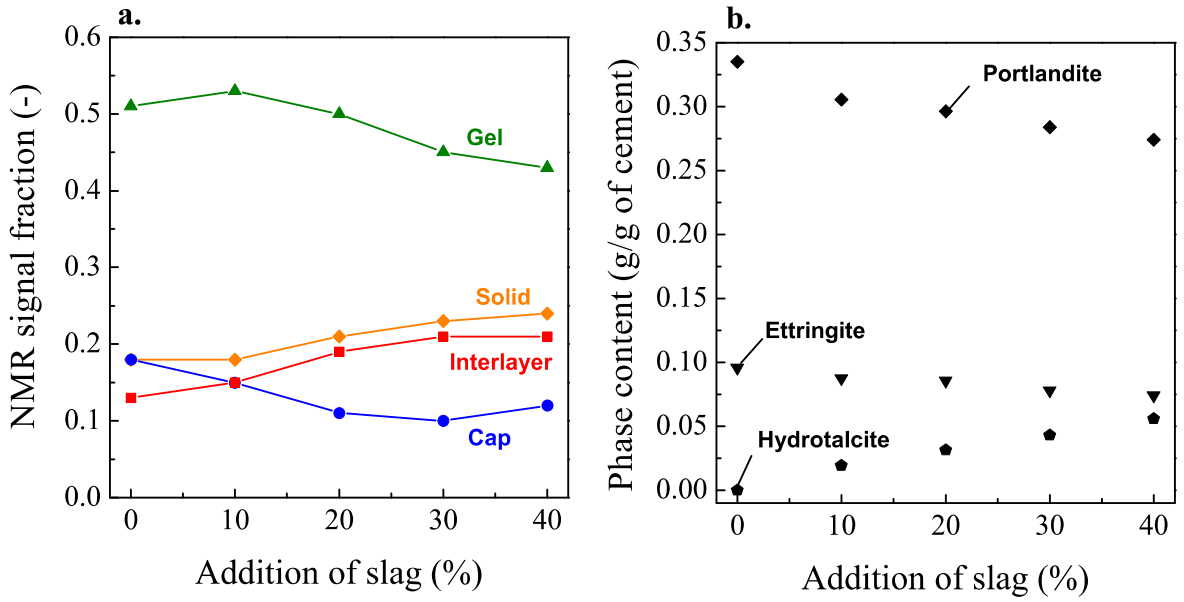

Figure 5 – (a) Different NMR signal fractions as a function of addition of slag after 28 days of hydration. (b) Crystalline phases content of Portlandite, Ettringite and Hydrotalcite in g/ g of cement as a function of slag addition.

Concerning the XRD results, we see a decrease of Portlandite and Ettringite as the slag content is increased. This correlates with the change in degree of hydration of cement (α_c) presented in table 1. Quartz favours the reaction of cement compared to slag and there is a difference of 10% in α_c between 40% of quartz and 40% of slag. As the specific surface area of both materials is similar, it highlights a competition between slag and cement dissolution. We also report the presence of Hydrotalcite when slag is present which increases up to 0.056 g/g of cement when 40% of slag is used. The different XRD crystalline phase contents shown in figure 5b were translated in terms of total water fraction in the mix based on their respective chemical composition and the way they bind water. The results are compared to the NMR signals I_{solid} in table 1. While there is a good agreement for 0 and 10% of slag addition, the values diverge for high replacements of slag. The difference in the favour of the NMR is explained by the precipitation of tricalcium-monosulfo-aluminate (Afm), seen by NMR but hardly detectable by XRD.

Table 1 – Degree of hydration of cement as a function of slag content. The NMR solid signal I_{solid} is also compared to the calculated water fraction bind in crystalline phases based on XRD results. Associated T_2 of interlayer water, gel water and capillary water spaces, in ms.

Slag content (%)	α_c	NMR I_{solid}	Calculated I_{solid} based on XRD	T_2 C-S-H interlayer (ms)	T_2 C-S-H gel (ms)	T_2 capillary (ms)
0%	0.88	0.18	0.19	0.086	0.409	1.25
10%	0.85	0.18	0.19	0.095	0.390	1.23
20%	0.82	0.21	0.19	0.101	0.386	1.50
30%	0.80	0.23	0.19	0.118	0.400	1.49
40%	0.78	0.24	0.19	0.122	0.404	1.49

Regarding NMR results, the addition of slag as a replacement of quartz increases the C-S-H interlayer signal and the signal associated to crystalline phases. This reflects the fact that despite the lower degree of hydration of cement when slag is used, more reactive material is present in the mix proportions. In parallel, more capillary water is consumed to form hydrates. The main change due to slag addition concerns the gel water fraction. Even if more C-S-H and crystalline phases are formed for high replacement levels of slag, the signal fraction I_{gel} becomes significantly smaller. The presence of slag does not favour the formation of gel pores and changes the way hydrates fill the space. We also report an increased amount of capillary water for 40% of slag replacement. Density calculations are needed to take further the analysis. This task is in progress as the degree of reaction of slag is required.

Concerning T_2 relaxation times reported in table 1, we report an increase in the interlayer T_2 value when more and more slag is added. In the same way, the T_2 of capillary water increases from 1.2 ms to 1.5 ms beyond 20% of slag content. More experiments are needed to confirm these trends as the slag introduces paramagnetic ions that can influence relaxation phenomena.

CONCLUSIONS

To conclude, we have developed a procedure to measure water locations in cement paste with ^{1}H NMR. Our methodology allows water mass quantification and calculation of pore sizes. Together, it brings the complete description of cement paste with crystalline phases content, C-S-H characteristics and pore size distribution. The impact of SCMs on the nanometric scale of cement porosity can be investigated for the first time. While silica fumes favours the gel pore formation, the slag has the opposite effect. Densities of C-S-H in the presence of 10% of silica fume are very similar to plain white cements with $\rho_x = 2.75$ g/cm^3 at 28 days for "solid" C-S-H density and $\rho_{x'} = 1.94$ g/cm^3 for "bulk" C-S-H density. However, the water content of C-S-H per mole of Si is lowered in the presence of silica fume, as well as the Ca/(Si+Al) ratio. While the size and amount of capillary water is little impacted by the presence of silica fume, the addition of 20% of slag

seems to increase the characteristic capillary pore size. The ^{1}H NMR technique has proven to be a powerful tool to characterize new material with a great level of detail on the nano-porosity of cement pastes. This can become a rapid mean to link microstructures to durability properties of concretes.

ACKNOWLEDGEMENTS

We thank Y.Q. Song of Schlumberger-Doll Research for 2D Fast Laplace Inversion software. White cement was provided by Aalborg Portland, Denmark. The research leading to these results has received funding from the European Union Seventh Framework Programme (FP7/2007-2013) under grant agreement 264448. P.J.M. thanks Nanocem (www.nanocem.org) and the UK Engineering and Physical Sciences Research Council (grant no. EP/H033343/1) for financial support. We also thank Jorgen Skibsted from Aarhus University for the ^{29}Si MAS NMR measurement and analysis.

REFERENCES:

1. World Business Council for Sustainable Development, Cement Sustainability Initiative, http://www.wbcsdcement.org, (accessed 1st December 2011).
2. R. Blinc M. Burgar, G. Lahajnar, M. Rozmarin, V. Rutar, J. Ursic,NMR Relaxation Study of Adsorbed Water in Cement and C3S Pastes" Journal of the American Ceramic Society, 61 (1978) 35-37
3. A. Valori, P.J. McDonald, K.L. Scrivener, The morphology of C–S–H: Lessons from 1H nuclear magnetic resonance relaxometry, Cement and Concrete Research (49) 65–81
4. W. P. Halperin, J.-Y. Jehng, Y.-Q. Song, Application of spin-spin relaxation to measurement of surface area and pore size distributions in a hydrating cement paste, Magnetic Resonance Imaging 12 (1994) 169 – 173
5. Meiboom, S.; Gill, D., Rev. Sci. Insts. 1958, 29, 688-691.
6. Powles, J. G.; Strange, J. H., Proc. Phys. Soc. London 1963, 82, 6-15.
7. Venkataramanan, L.; Song, Y.-Q.; Hürlimann, M. D. IEEE Trans. Signal Process 2002, 50, 1017-1026.
8. A.C.A. Muller, K.L. Scrivener, A.M. Gajewicz and P.J. McDonald, Densification of C-S-H measured by 1H NMR relaxometry, Journal of Physical Chemistry C 117 (2013) 403-412.
9. T. C. Powers, T. L. Brownyard, Studies of the physical properties 742 of hardened Portland cement paste; Portland Cement Association 743 (Bulletin 22): Chicago, 1948; reprinted from Proc. J. Am. Concr. Inst. 744 1947, 43, 101, 249, 469, 549, 669, 845, 993.
10. Jennings H. M. Refinements to colloidal model of C-S-H in cement: CM-II, Cem. Concr. Res., 38(3), 2008, 275-289.
11. A. J. Allen, J. J. Thomas & H. M. Jennings, Composition and density of nanoscale calcium–silicate–hydrate in cement, Nature Materials 6 (2007) 311-316
12. S.A. Rodger, et al., Microstructural developement during the Hydration of Cement. in Material Research Society Symposium Proceedings. 1987: Material Research Society.
13. E. Helsing Atlassi, Nonevaporable water and degree of cement hydration in silica fume-cement systems, in: V.M. Malhotra (Ed.), Proceedings of the 5th International Conference on Fly Ash, Silica Fume, Slag and Natural Pozzolans in Concrete, American Concrete Institute, Detroit (1995) 703–717
14. H. Justnes, E. J. Sellevold, G. Lundevall, High strength concrete binders. Part A: reactivity and composition of cement pastes with and without condensed silica fume', 4th International Conference on Fly Ash, Silica Fume, Slag and Natural Pozzolans in Concrete, Istanbul (1992) 873–889
15. S. Brunauer, S. A. Greenberg, The Hydration of Tricalcium Silicate and (ß-Dicalcium Silicate at Room Temperature, Proceedings of the 4th International Symposium on the Chemistry of Cement, Washington, Vol. 1(1960) 135–163
16. S. Bishnoi, K. L. Scrivener, μic: a new platform for modelling the hydration of cements, Cement Concrete Research 39 (2009) 266−274
17. W. Gutteridge, J. Dalziel, Filler cement. The effect of the secondary component on the hydration of portland cement: Part 1. A fine non-hydraulic filler, Cement and Concrete Research, 20 (1990) 778–782